ACS Sustainable Chemistry & Engineering

Research Article

pubs.acs.org/journal/ascecg

Functional Zein−Siloxane Bio-Hybrids

Letizia Verdolotti, Marino Lavorgna,* Maria Oliviero, Andrea Sorrentino, Valentina Iozzino, Giovanna Buonocore, and Salvatore Iannace

Institute for Composite and Biomedical Materials, National Research Council, P.le Fermi 1, Loc. Granatello, 80055 Portici, Naples, Italy

Supporting Information

ABSTRACT: Bio-hybrid films have been prepared by a sol−gel method starting from thermoplasticized zein (TPZ) and 3-glycidoxypropyltrimethoxysilane (GOTMS). A two-step procedure was adopted including the silane functionalization of zein macromolecules by reactive melting and the subsequent hydrolysis and condensation step of anchored GOTMS units with in situ formation of silsesquioxane (SSQO) nanostructures. These nanostructures bond the zein macromolecules with each other through the reaction of the GOTMS epoxy moieties with zein amine groups. Small angle X-ray scattering, transmission electron microscopy, and FTIR spectroscopy confirmed the formation of the hybrid network consisting of 2 nm-sized SSQO nanostructures dispersed in the zein matrix along with the modification of the hierarchical structure of zein. The organic−inorganic network induces an enhancement of mechanical and functional performances. In fact, owing to the presence of 3 wt % of siloxane as $SiO_{3/2}$, the maximum stress increases from 1.87 to 11.16 MPa, whereas the water uptake reduces from 100 to 20 wt % with respect to the neat TPZ. Furthermore, the bio-hybrids show an enhanced durability toward the biodegradation process.

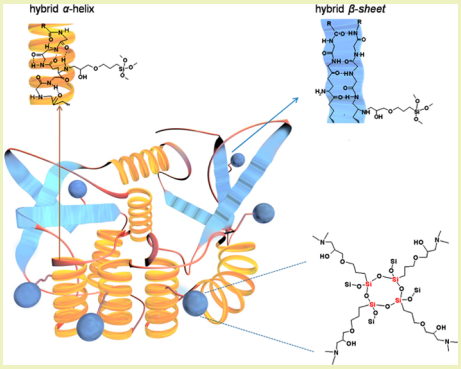

KEYWORDS: *Zein protein, SSQO domains, Bio-hybrid, SAXS/WAXD, Solid-state ^{29}NMR*

INTRODUCTION

During the last years, the use of agro-based protein sources has been recognized as one of the most promising approaches for substituting thermoplastic petrochemical-based polymers in several applications including food packaging, biomedical scaffolds, etc.

Among natural proteins zein found in corn endosperm, has been recently the object of research as well as industrial interest for its film-forming ability.[1,2] Furthermore, this material is available in large amounts as byproducts of agricultural and biofuel processing activities, for example, ethanol production.[1,2]

Corn zein has an amphiphilic character due to the fact that the main chain has polar amidic bonds but contains more than 50% nonpolar amino acids. This protein can be divided in two major fractions: α-zein, which includes about 80% of the available prolamine and is defined as the fraction being soluble in 95% ethanol, and β-zein, which is relatively unstable but is soluble in water.[2,3]

The main amino-acidic monomers of corn zein consist of glutamine (20−26%), leucine (21%), proline (10%), and alanine (10%).[4] However, compared to the conventional polymers, the materials from renewable sources present some disadvantages both in terms of processing and functional/structural performances. In particular, as already described by Oliviero et al.[5] and Zullo et al.,[6] natural biomaterials (such as starch and protein) show a limited thermal range of processability, as well as a lack of reproducibility mainly ascribed to the difficulty of controlling the molecular architecture and spatial conformation of natural macromolecules. In order to improve the thermal processing of zein, a suitable plasticizer, i.e., glycerol or polyethylenglycol, is used in combination with heat and shear. In this way, denaturation of the hierarchical structure of zein proteins causes a significant reduction in the extent of the hydrogen bonding network present in the neat zein.[7,8] With this method, known as thermoplasticization, the zein may be successfully formed into films and foams by compression molding, melt mixing, extrusion, and foaming processes. However, due to both the amphiphilic properties of the protein and the presence of plasticizer molecules, these materials show low thermal transitions, absorb large amounts of water, and are often subjected to migration of the plasticizer. Thus, compared to thermoplastic petrochemical-based polymers, they show lower physical and functional performances as well as limited industrial applications.[2] To overcome these restrictions, the inclusion of nanoparticles offers a suitable and valuable approach. A small amount of preformed nanoparticles such as nanoclays or fibrous clay[9] well-dispersed into the polymeric matrices, including zein, results in remarkable improvement in the mechanical, oxygen, and water vapor barrier,[10] and thermal

Received: August 14, 2013
Revised: October 8, 2013
Published: October 21, 2013

properties.[9−13] The nanometric inorganic particles can be also generated in situ by producing organic−inorganic hybrid materials. In detail, an inorganic network can be generated within the organic matrix from metal alkoxides, functionalized oligomers, and polymers by the sol−gel approach.[14,15] This led to a conceptually novel class of materials composed of both inorganic and organic domains in which highly tailored properties are achieved through careful control of their nanoscale interactions.[16,17]

A low-temperature procedure, high purity of reactants, and the possibility of mixing precursors of organic and inorganic phases at the molecular level are the main advantages of this technique. The alkoxysilane compounds $R_{(4-n)}Si(OR')_n$ are usually used as precursors of the inorganic phase by hydrolysis and condensation reactions. Linear or branched as well as cross-linked silsesquioxane ($RSiO_{3/2}$) are formed when trialkoxysilane is used as the starting material.[18]

Lee et al.[19] show that zein can be modified and strengthened by incorporation of highly stable silicate complexes obtained by hydrolysis and condensation of TEOS. The results confirm an increase in tensile strength from 7 to 14 MPa with 15 wt % of silica with a consequent reduction in the elongation at break and the increase in resistance to O_2 permeability. Similar results are obtained by Frost et al.[20] for thermoplastic starch−silica PVOH composite films obtained by a reactive extrusion process using TEOS as silica precursors.

In this paper, we prepare a bio-hybrid material from thermoplastic zein (TPZ) and 3-glycidoxypropyltrimethoxysilane (GOTMS) by a two-step procedure including reactive melt mixing and a simultaneous sol−gel approach. The hybrid structure consisting of silsesquioxane domains covalently bound to the zein macromolecules is achieved through simultaneous reactions between amines (from zein) and epoxy from GOTMS groups and hydrolysis and condensation of silane alkoxides moieties to produce siloxane domains. The occurrence of the reactions is verified by FTIR, whereas the morphology was investigated by small and wide angle X-ray scattering (SAXS/WAXS) and TEM analysis. Mechanical properties as well as chemico-functional properties in terms of water uptake and biodegradation are also evaluated in comparison to neat TPZ.

EXPERIMENTAL SECTION

Materials. Corn zein powder (CAS 9010-66-6, lot 065K0110, M_w = 25000 Da), poly(ethylene glycol), PEG (CAS 25322-68-3, M_w = 400 Da) used as plasticizer, and (3-glycidyloxypropyl)trimethoxy silane, GOTMS (CAS 2530-83-8, M_w= 236.34 Da) are purchased from Sigma-Aldrich, Italy. Calcium nitrate tetrahydrate (CAS 13477-34-4) is purchased from Carlo Erba, Italy. All of the materials are used as received from the suppliers.

Methods. *Preparation of TPZ-Based Hybrids.* Hybrid materials based on TPZ and GOTMS are prepared through a two-step process. The first process consists of preparing silane funtionalized materials by a reactive melt mixing method. Zein powder is added into the solution of PEG and GOTMS and mixed by using a spatula to provide a crude blend. PEG is 25 wt % of the zein and PEG system, whereas GOTMS is added in amounts to generate 1, 1.5, and 3 wt % of theoretical silica as $SiO_{3/2}$ with respect to the system of zein and PEG. The blend is then processed in a twin counter-rotating internal mixer (Rheomix 600 Haake, Germany) connected to a control unit (Haake PolyLab QC) for thermoplasticization. Mixing temperature, speed of rotation, and mixing time were 70 °C, 50 rpm, and 10 min, respectively, as reported by Oliviero et al.[8] Neat TPZ is subjected to the same mixing procedure for comparison. The materials obtained from this process are denoted as nhTPZ*x* with *x* equal to 1, 1.5, and 3 wt % to indicate the amount of theoretical silica as $SiO_{3/2}$.

In a second step, the materials extracted from the mixer are pressed at 80 °C and 50 MPa into films with a thickness of 0.5 mm by a hot press (P300P, Collin, Germany). The films are stored at room temperature and 50% RH in a closed box with a saturated salt solution of calcium nitrate to allow the generation of silsesquioxane domains by hydrolysis and condensation reactions of GOTMS. Hereafter, the hybrid materials after the hydrolysis process are denoted as TPZ*x*.

Characterization TPZ-Based Hybrids. *Solid-State ^{29}Si NMR.* Solid-state ^{29}Si NMR spectroscopy (^{29}Si-DPMAS-NMR) measurements are performed using a Bruker AV-300 apparatus. NMR spectra are obtained from 12,500 scans using the following parameters: rotor spin rate, 5000 Hz; recycle time, 5 s; contact time, 5 ms; and acquisition time, 33 h. Samples are packed in 4 mm zirconia rotors with KelF caps. Chemical shifts are relative to tetramethylsilane (TMS) using an external sample of tetrakis-trimethylsilyl-silane (TTMSS; upfield signal −135.4 ppm) as the secondary reference.

In the case of GOTMS, ^{29}Si NMR analysis provides quantitative data for the fractions of the structural T_n units, i.e., the structural units with *n* siloxane bonds (Si−O−Si) attached to the central atom and 3−*n* hydrolyzed groups (Si−OH). The assignment of the NMR bands was as follows: T_0 from −41 to −43 ppm, T_1 from −50 to −52 ppm, T_2 from −59 to −61 ppm, and T_3 from −66 to −69 ppm.[21] It is worth noting that the powder zein sample presents some silica impurities that give rise to the presence of Q_n units corresponding to Si atoms with *n* siloxane bonds (Si−O−Si) and 4−*n* hydrolyzed groups (Si−OH) that are in the range between −101 and −120 ppm.[22]

FTIR-ATR Spectroscopy. The chemical modifications induced by silsesquioxane structures on zein structures are evaluated by reflectance attenuate mode (ATR) FTIR spectroscopy. FTIR spectra for neat TPZ and hybrids are collected at room temperature by using a Nicolet apparatus (Thermo Scientific, Italy) from 4000 to 600 cm^{-1} with a wavenumber resolution of 4 cm^{-1} for 64 scans.

All spectra are baseline corrected following the Wellner method by ensuring that the spectrum was zeroed at 1800 cm^{-1} where the baseline was relatively horizontal[23] and normalized to the same height as the Amide II band.[24]

As reported in a previous paper,[4] the broad protein Amide I band can be decomposed into two components centered around 1658−1650 cm^{-1} and 1630−1620 cm^{-1} wavelengths assigned to the ordered α-helix and β-sheet phases, respectively, and a further band of around 1665−1675 cm^{-1} wavelengths ascribed to the unordered conformation, β-turns.[4,5,25]

Thus, the spectral region ranging from 1800 to 1600 cm^{-1} is deconvoluted with OriginPro 8.0 software by using Lorenzian functions, and the positions of the absorption bands corresponding to the different conformations (i.e., α-helix, β-sheet, and β-turns) are determined by an automatic peak-finding feature.[4,25,26]

Small Angle X-ray Scattering (SAXS). Structural characterization of neat TPZ and hybrid materials is performed through simultaneous WAXS and SAXS analyses by using an Anton Paar SAXSess instrument. All scattering data are corrected for the background and normalized for the primary beam intensity, whereas SAXS spectra were also additionally corrected for the Porod constant. The scattered beam intensity spectra was plotted as a function of the scattering vector *q* defined in eq 1

$$q = \frac{4\pi \sin\theta}{\lambda} \quad (1)$$

where θ is the scattered angle and λ is the wavelength of the X-rays of Cu Kα (i.e., 0.154 nm).

Transmission Electron Microscopy (TEM). The morphological structures of films are characterized using a TEM-100CX apparatus manufactured by JEOL. Examinations are made on thin slices microtomed from cast films embedded in epoxy resin.

Thermogravimetry Analysis (TGA/DTG). The thermal degradation of materials is investigated by thermogravimetric (TGA) analysis. The tests are carried out by using a TGA2950 (TA Instruments, U.S.A.)

under air atmosphere. The samples are heated from 30 °C up to 1000 °C by applying the heating rate equal to 10 °C/min.

Mechanical Properties. The tensile properties in terms of maximum stress, σ_M, and strain at break, ε_B, are measured at room temperature with a 1 kN load cell by using an Instron model 4204 tensile test machine according to ASTM D 1708-02. In order to assess the formation of organic−inorganic networks, the mechanical properties of five samples for each composition are tested both before and after hydration process, and the average values are reported.

Water Uptake and Solubility Resistance Test. The effects of the presence of hybrid organic−inorganic structures on water uptake, weight loss in water by PEG leaching, and solubilization in ethanol are also assessed.

Weight loss for PEG leaching and water uptake are evaluated on samples (2 cm × 2 cm) dried under vacuum for 24 h at 25 °C. Subsequently, the samples are immersed at room temperature in distilled water and extracted at regular time intervals: 3, 6, 9, 12, 25, 120, and 240 min. The surfaces of the samples are gently wiped, and then the samples are weighted. Finally, the films are dried at 25 °C under vacuum up to constant weight.

The weight loss of the samples (WL) is calculated as

$$\mathrm{WL}\ (\%) = \frac{M_0 - M_{\mathrm{df}}}{M_0} \times 100 \qquad (2)$$

where M_{df} is the weight of dry sample after immersion in water for a time interval t, and M_0 is the dry weight before immersion in water.

The water uptake (WU) is calculated as

$$\mathrm{WU}\ (\%) = \frac{(M_t - M_0) + (M_0 - M_{\mathrm{df}})}{M_0} \times 100 \qquad (3)$$

where M_t is the weight of wet sample at time t, and M_0 is the weight of dry sample before the immersion in water.

In order to analyze the effect of silsesquioxanes on TPZ, solvent resistance solubility tests are performed for neat TPZ and hybrids by immersing the samples in ethanol (96% aqueous alcohol)[27] for 25 min at 90 °C with a film/ethanol ratio equal to 1/48 (w/w) lower than the limit of solubility of zein[1,2] and assessing their capability to resist ethanol dissolution.

Biodegradation Test. The biodegradation rate in controlled composting conditions (according to ASTM D5338 and ISO 14855 standards) of the samples is evaluated by a respirometric system developed at the University of Salerno.[28] The compost used, coming from municipal waste, is kindly supplied by the AMA plant in Maccarese (Rome). Cellulose in powder form is used as a positive control. The test materials are prepared by cutting the film samples into squares with a surface of about 10 mm × 10 mm with a thickness of about 0.2 mm.

A mixture of mature compost (600 g, wet weight) and test materials (100 g, wet weight) is introduced into a static reactor vessel where it is incubated at 58 °C.

The moisture content in the compost is controlled to be in the range of 50−60%. pH is as low as 7 in the initial stage of the composting, and naturally increased to around 8.0 as the composting progressed due to ammonification of nitrogen components in the compost.

The total dry solids content is obtained by taking a known amount of test material and drying it at 105 °C to a constant weight. The volatile solids on dry weight are calculated by subtracting the residues of a known amount of test material after incineration at 550 °C from the total dry solids content of the same sample and relating that to the total solids content of the compost.

Carbon dioxide produced from both the test material and the compost is continuously monitored and integrated to determine the rate and cumulative carbon dioxide production. After determining the carbon content of the test compound, the percentage of biodegradation is calculated as the percentage of solid carbon of the test compound that has been converted to CO_2.

The theoretical carbon content of the test compound $(CO_2)_{th}$ is determined from the chemical composition of each and the relative amount of sample components (zein, PEG, and GOTMS). In particular, using the amino acid composition of zein, the amount of carbon in the zein is 13007.6 g/mol/27144 g/mol = 47.9%. Percent biodegradation, as mineralization (%) is then calculated from

$$\mathrm{mineralization} = \frac{(CO_2)_{\mathrm{compost+zein}} - (CO_2)_{\mathrm{compost}}}{(CO_2)_{\mathrm{th}}} \times 100 \qquad (4)$$

where $(CO_2)_{compost+zein}$ is the average CO_2 production from the composter with investigated samples, and $(CO_2)_{compost}$ is the average CO_2 production from the only composter.

RESULTS AND DISCUSSION

Thermoplasticization of Zein. Figure 1 shows the evolution of torque versus time during the mixing process for neat TPZ and the nhTPZ1.5 and nhTPZ3 systems. Typically, the curves obtained during thermoplasticization of protein−plasticizer systems[29] are characterized by an initial induction time followed by a steep increase in torque to a maximum and then a continuous decrease to a rather stationary value when the melt temperature becomes constant. As shown in Figure 1, for all systems, the torque increases immediately with an absence of the induction time. This result suggests that the diffusion of plasticizer within the protein macromolecules is favored by the presence of silane. However, after plasticization, the value of the torque is rather constant only for nhTPZ, while for the nhTPZ1.5 and nhTPZ3 systems the torque increases. This is ascribed to the chemical reaction between epoxy-GOTMS and amino groups of zein, which results in increasing branching and the molecular weight of protein macracomolecules. Moreover, as discussed below, during the thermoplasticization process, cross-linking reactions also occur involving the formation of siloxane bonds and silsesquioxanes structures. In this respect, the cross-linking effect due to the displacement of the silane ethoxy groups by hydroxylic groups present on specific aminoacids (i.e serine and tyrosine) within zein macromolecules cannot be neglected.

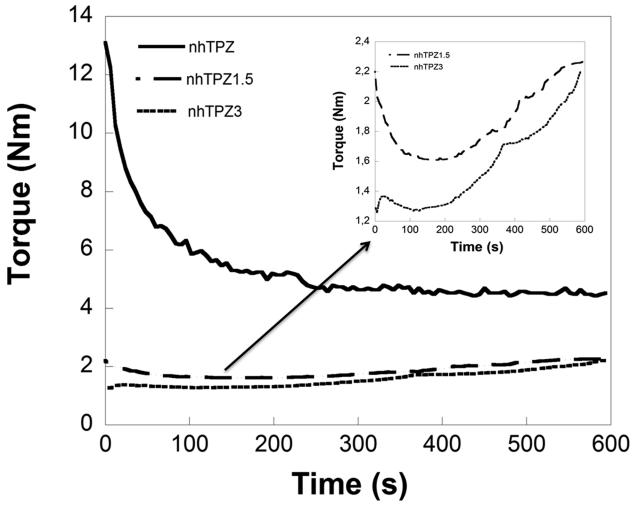

Figure 1. Torque evolution during the mixing process for the nhTPZ, nhTPZ1.5, and nhTPZ3 systems.

Another interesting feature is that the value of torque is always lower for hybrid samples during the whole mixing process. This behavior is attributed to the plasticizing effect of GOTMS molecules.

Chemical Characterization of TPZ-Based Hybrids. Solid-state ^{29}Si NMR spectroscopy is a useful technique to investigate the structure of the inorganic phase during the formation of hybrid materials. The ^{29}Si NMR spectra for nhTPZ3 and TPZ3 samples, reported in Figure 2, exhibit two

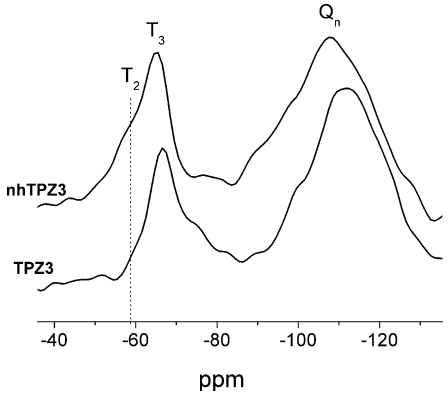

Figure 2. ^{29}Si NMR spectra for nhTPZ3 and TPZ3 samples.

broad signals in the regions from −50 to −70 ppm and −90 to −120 ppm assigned, respectively, to the T_n and Q_n structures. In particular, in the region of T_n structures, the resonance bands at −59 and −65 ppm ascribed, respectively, to T_2 and T_3 structures are clearly identified. As a consequence of the hydrolysis and condensation reactions occurring during the hydration process, the intensity of the T_2 resonance band decreases, whereas other bands at higher resonance values appear to confirm the presence of a large population of siloxane structures. The presence of Q_n structures, quite unexpected, is ascribed to the presence of some silica residues coming from the zein extraction from corn materials (^{29}Si NMR spectrum is located in the Supporting Information). It is worth considering that the probable displacement of ethoxy groups of GOTMS units anchored to zein macromolecules by hydroxyl groups of specific aminoacids, i.e., serine and tyrosine, may bring the formation of several structures around the silicon atoms with a consequent shift of the T_n signals to higher resonance values. This explains the presence of an additional band at −75 ppm as well as the broadening of the Q_n peak observed for the TPZ3 sample. These results confirm that silsesquioxane structures form during the reactive melting process, and the successive hydration process carried out by storing the hybrid samples in a humid environment contributes to better structuring of the siloxane domains.

Deep understanding of the chemical modifications occurring to the zein structure by the interactions with GOTMS and with silsesquioxanes structures can be derived from infrared spectroscopy.[5,30]

Figure 3 shows the FTIR spectra of neat TPZ, nhTPZ3, and TPZ3 alongside the bands by deconvolution of the Amide I peaked at 1624, 1652, and 1676 cm^{-1} wavenumbers assigned, respectively, to β-sheet, α-helix, and β-turn conformations (other spectra are not reported for brevity).[4,5,25]

FT-IR spectra of nhTPZ3 and TPZ3 films show distinct absorption bands around 1200 cm^{-1} related to the Si−CR stretching vibration[31] where R is the side chain of GOTMS. The absorption band of oxirane expected at 910 cm^{-1} is not detected because it reacts with the amine groups present in the zein primary aminoacids (glutamine, aspargine, histidine, and arginine).

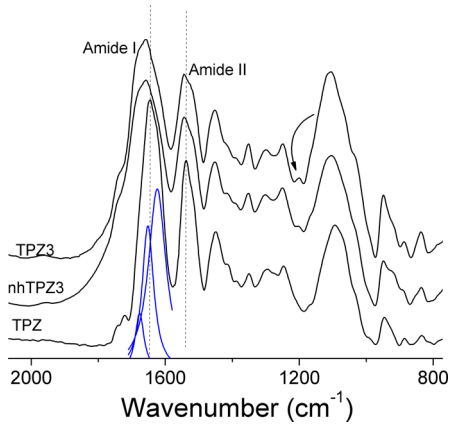

Figure 3. FTIR spectra of TPZ, nhTPZ3, and TPZ3.

By analyzing the absorption bands of Amide I and Amide II, it is noted that the presence of silsesquioxane domains brings a shift in the frequencies and a broadening of the band area. In particular for Amide II, the vibration frequencies increase from 1537 cm^{-1} for TPZ to 1543 cm^{-1} and 1545 cm^{-1} for nhTPZ3 and TPZ3, respectively. This shift is attributed to the formation of new bonds between the GOTMS epoxy group with the N−(R) of polypeptide that modifies the chemical neighborhood of Amide II.

Similar results are also noted by Athamneh et al.[4] for several proteins plasticized with glycerol. They observed that the Amide II band position shifted to a higher frequency (for all of the proteins) for a high amount of glycerol because the hydrogen interactions glycerol−glycerol and protein−protein were favored. Conversely, at low glycerol concentrations, these interactions decreased, and glycerol−protein interactions occurred with a consequent shift of the Amide II band position.

Relating to Amide I, the presence of silsesquioxanes brings a significant modification of the secondary conformations (i.e., β-sheet, α-helix, and β-turn) as confirmed by the shifting of the vibration frequencies observed for nhTPZ3 and TPZ3 to higher values with respect nhTPZ (data are reported in Table 1).

An overall understanding of the occurrence of modifications can be obtained by the ratio of ordered phases (α-helix and β-sheet) to disordered phases (β-turns) defined as follows

$$R = \frac{(A_{\alpha\text{-helix}} + A_{\beta\text{-sheet}})}{A_{\beta\text{-turns}}} \quad (5)$$

where $A_{\alpha\text{-helix}}$, $A_{\beta\text{-sheet}}$, and $A_{\beta\text{-turns}}$ are, respectively, the band area obtained by the deconvolution of spectra for the α-helix, β-sheet, and β-turns conformations.

The data are reported in Table 1, and a decrease in R for nhTPZ3 and TPZ3 with respect to the TPZ is observed. The decrease in ordered secondary conformations can be ascribed to the formation of the hybrid silsesquioxane−zein structures that affect the initial arrangements of the secondary structure of neat TPZ.

The siloxane domains typically give infrared absorption bands in the vibration regions of 1100−1000 cm^{-1} and 950−900 cm^{-1} assigned to Si−O−Si and Si−OH, respectively. In the spectra reported in Figure 3, the Si−OH stretching vibration band can be observed as a shoulder of a main absorption band of TPZ that disappears due to the hydration process. Furthermore, the vibration band at 1100−1000 cm^{-1}, attributed to the stretching of the ether group (C−O−C linkage) for neat

dx.doi.org/10.1021/sc400295w | ACS Sustainable Chem. Eng. 2014, 2, 254−263

Table 1. FTIR Data

	Amide I peak position (cm^{-1})					
sample	α-helix	β-sheet	β-turn	others	$(A_{\alpha\text{-helix}}+A_{\beta\text{-sheet}})/A_{\beta\text{-turn}}$	Amide II peak position (cm^{-1})
nhTPZ	1652	1624	1676	–	7	1537
nhTPZ3	1662	1642	1682	1734	5	1543
TPZ3	1667	1647	1689	1742	4	1545

TPZ, show both a significant shift at higher wavenumbers and an intensity increase due to the formation of Si−O−Si linkages.

Morphological Characterization of TPZ-Based Hybrids. As reported by several authors,[32] the molecular aggregates in the zein powder do not present diffraction patterns over the small-angle range because they do not have long-range periodicity. However, when the zein is plasticized with compounds, PEG scattering features are observed because the arrangement of molecules into a long-range periodic is a facilitated mechanism.[29]

SAXS and WAXD patterns of neat TPZ, TPZ1.5, and TPZ3 are shown in Figure 4. The WAXD pattern of neat zein displays

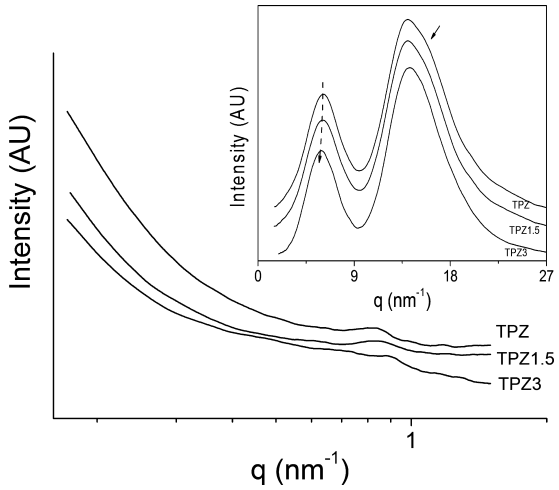

Figure 4. SAXS patterns for TPZ, TPZ1.5, and TPZ3 films. WAXD patterns are reported in the inset graphs.

two diffraction peaks at q values of 6 and 14 nm ascribed, respectively, to the packing of neighbors of α-helixes and the average backbone distance within the α-helixes (Figure 4, inset).

The diffraction patterns are affected by the presence of hybrid organic−inorganic structures. The peak related to the α-helix packing slightly shifts to lower scattering q vector values confirming a slight increase in the separation distance between the α-helix, whereas the peak of higher q values became more symmetric. As for the SAXS analysis, TPZ exhibits both a diffraction feature at 0.85 nm^{-1} due to the arrangement of zein molecules and PEG into a long-range periodic structure and an upturn intensity at low scattering vectors due to presence of large zein molecule aggregation.[32,33]

As a consequence of the addition of GOTMS, the TPZ3 sample shows a reduction in the diffraction feature associated to the long-range periodic structure alongside an evident reduction in intensity diffracted by large zein aggregates. These results confirm that the hybridization process modifies the hierarchical structure of zein affecting the α-helix conformation as well as the large aggregates (i.e., third and quaternary morphology). A schematic representation of modifications that take place during hybridization is reported in Scheme 1 The TEM micrographs related to neat TPZ and TPZ hybrid films are reported in Figure 5. The TEM image of TPZ shows the presence of inhomogeneous morphology with clear zones alternating to denser zones. This may be ascribed to the segregation of PEG between zein macromolecules. Conversely, the micrograph of the hybrid sample shows some dense domains, 2 nm sized.[34].

Thermal, Mechanical, and Functional Characterization of TPZ-Based Hybrids. Table 2 summarizes the thermal degradation data for the several stages identified by thermogravimetric analysis for TPZ and hybrids samples. The residue at 800 °C is also reported. The thermograms of neat TPZ show three decomposition steps.[13] The first and second stages corresponds to the degradation of several zein polypeptides with different molecular weights, while the third stage corresponds to the loss of volatile compounds produced during the first stages.

As reported by several authors,[9,35] the thermal stability of the polymer can be assessed through the temperature at which a weight loss of 20% occurred. As reported in Table 2, the temperature at 20% weight loss increases with respect to neat TPZ by increasing the silsesquioxanes content. In accordance with the literature,[9] the presence of inorganic nanodomains delays the decomposition process acting as a thermal barrier isolating the inner flammable gases and the outside oxygen and heat.[12,36]

The residue at 800 °C provides a rough estimation of silica filler. It is about 1.6 wt % for TPZ1.5 and 3.6 wt % for TPZ3, thus confirming that the silica content is similar to the expected theoretical silica content. The residue of TPZ is ascribed to the presence of silica particles as an impurity according to the ^{29}Si NMR results (^{29}Si NMR spectrum is located in the Supporting Information).

The stress−strain curves for neat TPZ and the TPZ-based hybrid with 3 wt % of silsesquioxane domains before and after the hydration process are shown in Figure 6. Trends in stress−strain curves for the other systems are similar and are not reported for simplicity. Tensile properties are summarized in Table 3. From Figure 6, it is observed that before the hydration process nhTPZ3 has a higher value of maximum stress, σ_M, and a slight lower value of elongation at break, ε_B, than nhTPZ. The improvement of mechanical properties by adding an inorganic component is ascribed to the cross-linking of zein macromolecules achieved as a result of the reaction during reactive melt mixing between GOTMS and the zein protein. After the hydration process, changes in the mechanical properties are observed for both TPZ and the TPZ-based hybrid. The σ_M increases by about 65% from 1.87 to 5.4 MPa for neat TPZ and by about 80% from 2.2 to 11.16 for the hybrid with 3 wt % of silsesquioxane domains. Conversely, the elongation at break values shows a decrease after the hydration process. The increase in σ_M and decrease in ε_B for neat TPZ is attributed to the migration phenomenon of PEG toward the exterior of the films. Various authors[37,38] have investigated the changes in the

Scheme 1. Schematization of Zein Structure (a) Before and (b) After Reaction with GOTMS and Formation of Silsesquioxane Domains

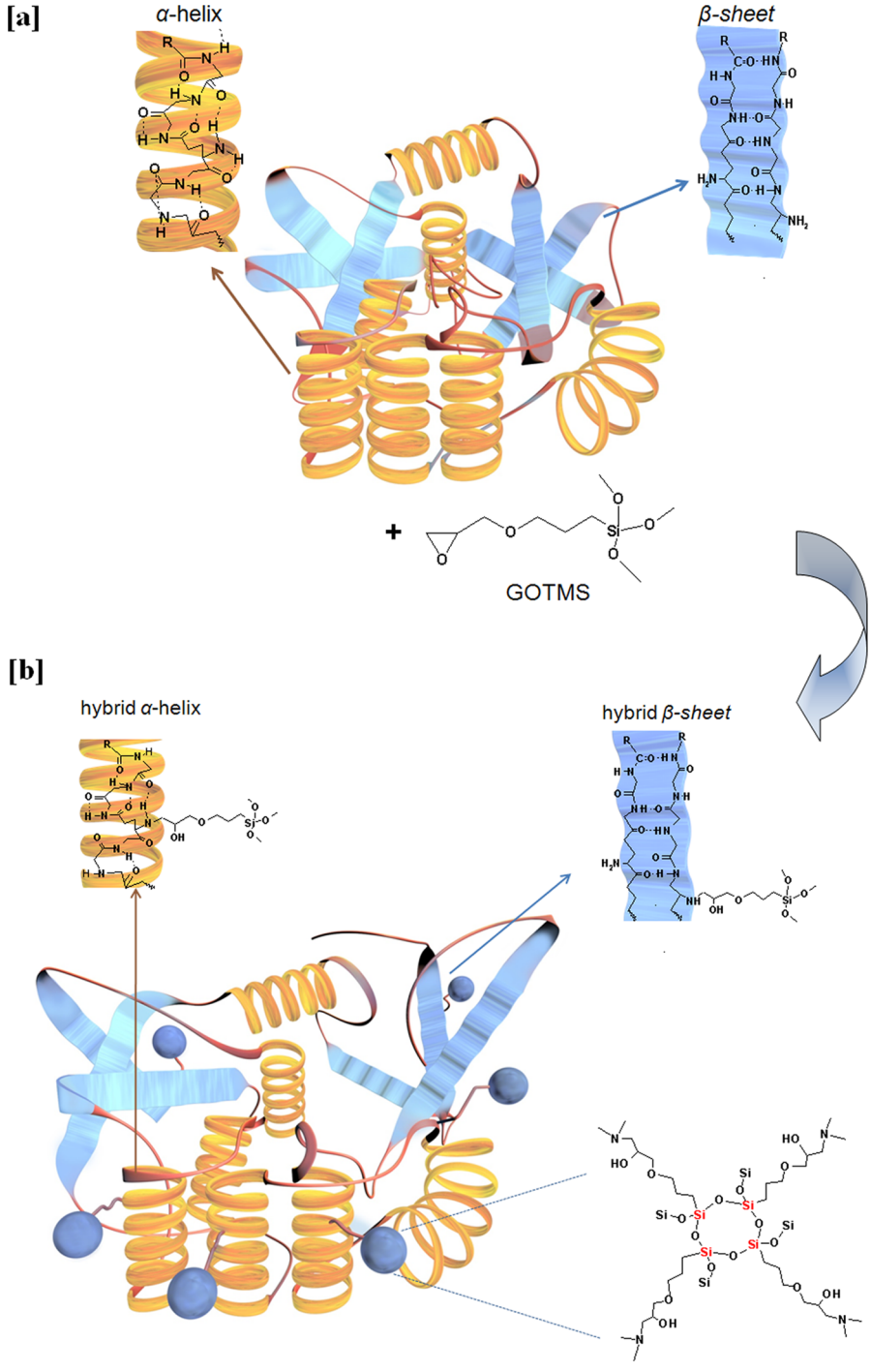

mechanical properties of plasticized protein-based films over time. Orliac et al.[39] studied the effect of various plasticizers and aging conditions on mechanical properties for sunflower films. They showed that a large amount of plasticizer was lost within 24 days and concluded that the films became rigid due to an increase in the number of interactions between protein chains in the absence of a plasticizer. Compared with TPZ, TPZ-based films containing inorganic domains are more prone to became rigid in the hydration process, as shown by their mechanical properties (Table 3). This behavior is ascribed to the plasticizer migration as well as the occurring cross-linking by formation of silsesquioxane domains. Similar results have been reported by Lee et al.[40] for films of corn zein modified with silica by a sol–gel technique. The authors observe, however, only a 50% increase in σ_M with the addition of 15 wt % silica. In our work, a remarkable improvement was observed even at lower silica content. The effectiveness of the sol–gel approach to improve the mechanical properties of TPZ can be confirmed through a comparison among our results and those reported by Oliviero et al.[5] for zein-based nanocomposites with different kinds of preformed particles in different contents. The authors reported a comparison among the mechanical properties, expressed as

dx.doi.org/10.1021/sc400295w | ACS Sustainable Chem. Eng. 2014, 2, 254–263

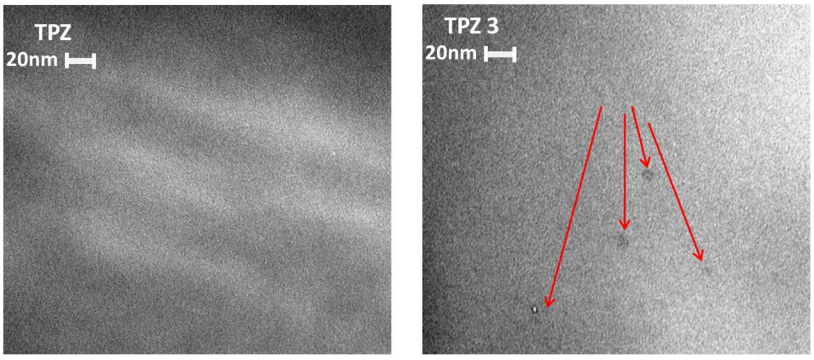

Figure 5. TEM micrographs of TPZ and TPZ3.

Table 2. TGA and DTGA Results

sample	T_{d1} (°C)	T_{d2} (°C)	T_{d3} (°C)	T at 20% of weigth loss (°C)	residue at 800 °C (wt %)	theoretical $SiO_{3/2}$ (wt %)
TPZ	327	410	506	295	0.5	0
TPZ1.5	326	415	513	300	1.60	1.5
TPZ3	327	423	623	310	3.60	3

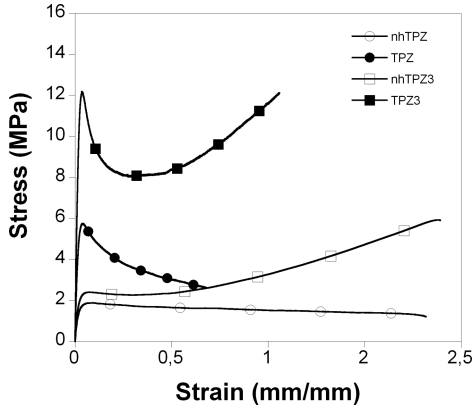

Figure 6. Stress–strain curves before and after hydration process.

relative values with respect to the neat system of TPZ–alkaline lignin nanocomposites and of zein–montmorillonite nanocomposites found in the literature prepared by solvent casting, film blowing of a resin obtained by the precipitation of zein from an aqueous ethanol solution, and melt mixing methods. The comparison among data clearly provide evidence of the high efficiency of inorganic nanodomains with respect to the use of preformed fillers even for low silica contents. A relative σ_M of 6 has been calculated for the TPZ3 system with respect to a maximum value of 3.2 obtained for TPZ-based nanocomposites with 10 wt % of filler.

The kinetic of water uptakes for TPZ and hybrids, TPZ1.5 and TPZ3, are reported in Figure 7a. In Figure 7b, the weight loss registered after water immersion that represents a rough estimation of the tendency to PEG leaching is reported, also.

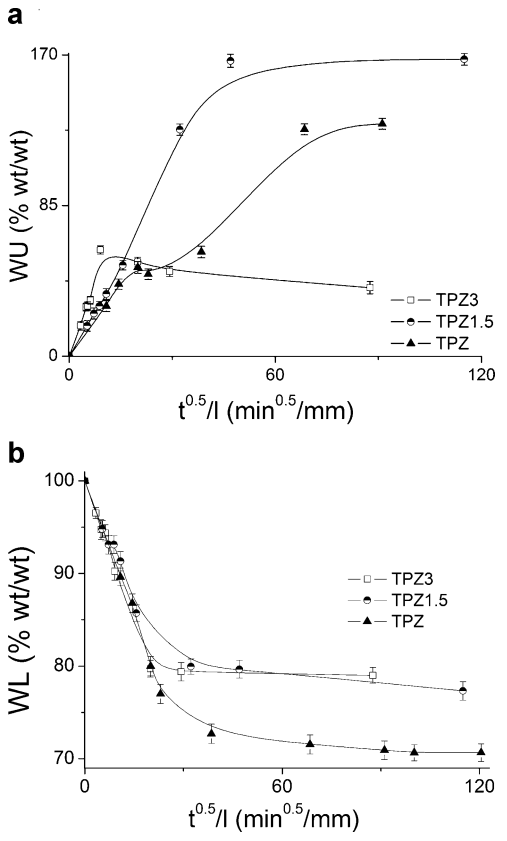

Figure 7. (a) Water uptake of TPZ, TPZ1.5, and TPZ3. (b) Weight loss of TPZ, TPZ1.5, and TPZ3.

The results show that the presence of about 3 wt % silsesquioxane domains reduces the water uptake significantly

Table 3. Tensile Properties before and after Hydration Process

sample	σ_M (MPa)	σ_B (MPa)	ε_B (%)
nhTPZ	1.8775 ± 0.43	1.2598 ± 0.51	180 ± 11.4
nhTPZ1.5	3.6444 ± 0.5614	2.3547 ± 0.6565	137.4164 ± 10.3975
nhTPZ3	2.2382 ± 0.6528	5.6336 ± 1.0517	191.8527 ± 14.5692
TPZ	5.4164 ± 0.3416	2.5815 ± 0.5180	60.7575 ± 12.9093
TPZ1.5	8.8223 ± 1.0964	4.8676 ± 0.7888	83.75 ± 13.0896
TPZ3	11.1617 ± 1.4785	11.2585 ± 1.2288	106.7515 ± 8.1530

dx.doi.org/10.1021/sc400295w | ACS Sustainable Chem. Eng. 2014, 2, 254–263

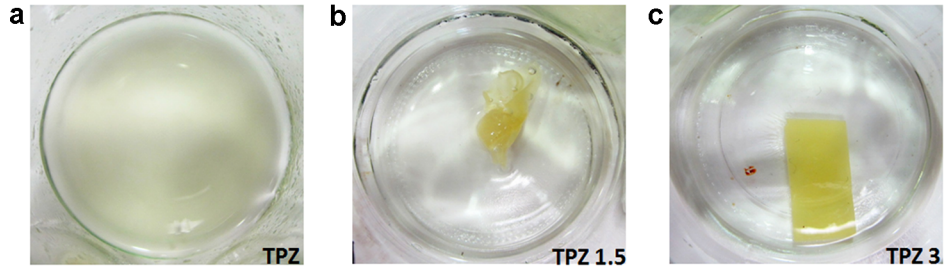

Figure 8. Samples after solubility test in ethanol: (a) TPZ, (b) TPZ1.5, and (c) TPZ3.

and improves the retention of PEG during immersion in water with respect to neat TPZ.

In particular, it is worth noting that the kinetics of water uptake depends on the material. TPZ and TPZ1.5 show a sigmoidal sorption trend attributed to the diffusion process controlled by the accumulation of water on specific sites. Then the materials start to swell, and the water penetrates, whereas the plasticizer migrates through the external surface. The absorption kinetic showed by TPZ3 rises rapidly to equilibrium through a maximum. Similar results are reported by Mascia et al.,[34] where they ascribe this behavior to a reduction in free volume due to physical aging.[34]

The results confirm that when the inorganic content is around 3 wt %, the silsesquioxane domains and extent of organic−inorganic cross-linking limit the swelling of the material and/or the PEG migration making the material not soluble in ethanol. Conversely, neat TPZ and TPZ 1.5, respectively, solubilized in a few minutes and swelled a significant extent (Figure 8).

Biodegradation test is evaluated on selected samples TPZ, TPZ1.5, and TPZ3. In general, the process of aerobic degradation comprises two phases: disintegration and mineralization. The initial phase, or disintegration, is significantly associated with the macroscopic properties of the material, such as permeability, density, mechanical properties, and specimen dimension. The second phase, or mineralization, occurs when living organisms digest the organic products of the initial phase and convert them to simple molecules (CO_2, water, and cell biomass). The initial phase is related to the initial time lag shown by the mineralization curves, whereas the rate and amount of biodegradation reached is associated to the second phase.

The results obtained by monitoring the rate and amount of produced CO_2 by the analyzed samples are exhibited in Figure 9. As expected, TPZ and cellulose are easily mineralized to CO_2 by the compost in a few days. The biodegradation of cellulose started almost immediately at a high rate and reached 80% in about 15 days. Differently, the TPZ shows about five days of initial time lag. After about 25 days, the biodegradation of the TPZ reached a maximum value of about 78%. This level of degradation is similar to that found for other similar protein-based polymers.[41,42] The presence of SSQO nanostructures strongly delay the biodegradability of samples decreasing both the rate and maximum biodegradation value reached. In particular, the sample containing 1.5 wt % of theoretical $SiO_{3/2}$ shows a similar initial time lag of the pure zein but shows a slow degradation rate. A high level of GOTMS strongly delays the biodegradation process. After about 25 days, the sample containing 3 wt % of SSQS showed no biodegradation at all. At this point, the biodegradation starts quickly up to the same biodegradation percentage reached by the sample containing

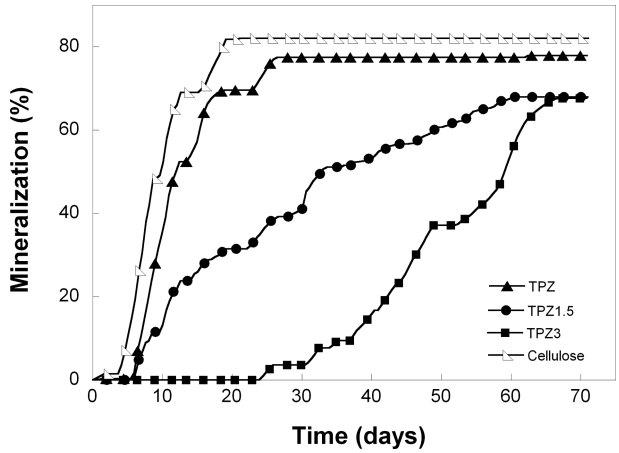

Figure 9. Evolution of biodegradation of cellulose, thermoplasticized zein, and hybrid films in compost.

1.5 wt % of SSQS (about 67%). The cross-linked network in hybrid samples hindered the penetration of degrading enzymes into polymer gels therefore significantly delaying the first step of biodegradation.

These results suggest that the degradation rate of TPZ can be tailored by changing the cross-link density. The possibility of varying the biodegradation rate makes the hybrid materials suitable for applications in which biodegradation is desired only after a certain period. This might be of particular interest for use in plastics for packaging or soil applications.

CONCLUSIONS

Bio-hybrid materials have been obtained by a sol−gel method from PEG thermoplasticized zein and 3-glycidoxypropyltrimethoxysilanes that generate silsesquioxanes structures as chemical cross-linking between zein macromolecules. The materials are designed to establish cross-linking bonds by the reaction of glycidoxy groups with amines of zein aminoacids as well as by the displacement of ethoxy silane groups by hydroxyl groups of peculiar zein aminoacids. Structural and morphological characterizations by a wide range of techniques (^{29}Si NMR, FTIR, SAXS, WAXS, and TEM) confirm the obtainment of a hybrid structure consisting of small inorganic domains homogeneously dispersed throughout the material and covalently linked to the organic macromolecules. The results confirm that the sol−gel approach modifies only slightly the secondary structure of zein proteins. However, the hybrids show an interesting combination between enhanced mechanical properties, reduced water uptake, and increased resistance to swelling as well as dissolution in boiling solvents. The cross-linked structure enhances the resistance of hybrids toward the biodegradation process.

dx.doi.org/10.1021/sc400295w | ACS Sustainable Chem. Eng. 2014, 2, 254−263

■ ASSOCIATED CONTENT

Supporting Information

Figure SI is the ^{29}Si NMR of neat zein powder. The band at ~111 ppm is ascribed to the Q_n structures associated with the presence of silica as the impurity in the material. This material is available free of charge via the Internet at http://pubs.acs.org.

■ AUTHOR INFORMATION

Corresponding Author

*E-mail: mlavorgn@unina.it. Tel: +39 081 775 8838. Fax: +39 081 775 8850.

Notes

The authors declare no competing financial interest.

■ ACKNOWLEDGMENTS

This work was supported by the Italian Ministero dell'Istruzione, dell'Università e della Ricerca (MIUR), within the framework of FIRB under Grant RBPR05JH2P "ITALNANONET". We are grateful to Fabio Docimo for technical support and Enza Migliore for drawing support.

■ REFERENCES

(1) Lawton, J. W. Zein: A history of processing and use. *Cereal Chem.* **2002**, *79*, 1−18.
(2) Shukla, R.; Cheryan, M. Zein: The industrial protein from corn. *Ind. Crops Prod.* **2001**, *13*, 171−192.
(3) Mahal, A.; Khullar, P.; Kumar, H.; Kaur, G.; Singh, N.; Jelokhani-Niaraki, M.; Bakshi, M. S. Green chemistry of zein protein toward the synthesis of bioconjuate nanoparticle: Understanding unfolding, fusogenic behavior, and hemolysis. *Sustain. Chem. Eng.* **2013**, *1*, 627−639.
(4) Althamneh, A. I.; Griffin, M.; Whaley, M.; Barone, J. R. Conformational changes and molecular mobility in plasticized proteins. *Biomacromolecules* **2008**, *9*, 3181−3187.
(5) Oliviero, M.; Verdolotti, L.; Aurilia, M.; Di Maio, E.; Iannace, S. Effect of supramolecular structures on thermoplastic zein−lignin bionanocomposites. *J. Agric. Food Chem.* **2011**, *59*, 10062−10070.
(6) Zullo, R.; Iannace, S. The effects of different starch sources and plasticizers on film blowing of thermoplastic starch: Correlation among process, elongational properties and macromolecular structure. *Carbohhyd Polym.* **2009**, *77*, 376−383.
(7) Di Maio, E.; Mali, R.; Iannace, S. Investigation of thermoplasticity of zein and kafirin proteins: Mixing process and mechanical properties. *J. Appl. Polym. Sci.* **2010**, *18*, 626−633.
(8) Oliviero, M.; Di Maio, E.; Iannace, S. Effect of molecular structure on film blowing ability of thermoplastic zein. *J. Appl. Polym. Sci.* **2010**, *115*, 277−287.
(9) Alcântara, A. C. S.; Darder, M.; Aranda, P.; Ruiz-Hitzky, E. Zein−fibrous clays biohybrid materials. *Eur. J. Inorg. Chem.* **2012**, 5216−5224.
(10) Ozcalika, O.; Tihminlioglu, F. Barrier properties of corn zein nanocomposite coated polypropylene films for food packaging applications. *J. Food Eng.* **2013**, *114*, 505−513.
(11) Luecha, J.; Sozer, N.; Kokini, J. L. Synthesis and properties of corn zein/montmorillonite nanocomposite films. *J. Mater. Sci.* **2010**, *45*, 3529−3537.
(12) Alexandre, M.; Dubois, P. Polymer-layered silicate nanocomposites: Preparation, properties and uses of a new class of materials. *Mater. Sci. Eng., R* **2000**, *28*, 1−63.
(13) Nedi, I.; Di Maio, E.; Iannace, S. The role of protein−plasticizer−clay interactions on processing and properties of thermoplastic zein bionanocomposites. *J. Appl. Polym. Sci.* **2012**, *155*, E314−E323.
(14) Mascia, L.; Prezzi, L.; Willox, G. D.; Lavorgna, M. Molybdate doping of networks in epoxy−silica hybrids: Domain structuring and corrosion inhibition. *Prog. Org. Coat.* **2006**, *56*, 13−22.
(15) Lavorgna, M.; Gilbert, M.; Mascia, L.; Mensitieri, G.; Scherillo, G.; Ercolano, G. Hybridization of Nafion membranes with an acid functionalised polysiloxane: Effect of morphology on water sorption and proton conductivity. *J. Membr. Sci.* **2009**, *330*, 214−226.
(16) Pandey, S.; Mishra, S. B. Sol−gel derived organic−inorganic hybrid materials: Synthesis, characterizations and applications. *J. Sol-Gel Sci. Technol.* **2011**, *59*, 73−94.
(17) Piscitelli, F.; Lavorgna, M.; Buonocore, G.; Verdolotti, L.; Galy, J.; Mascia, L. Plasticizing and reinforcing features of siloxane domains in amine-cured epoxy/silica hybrids. *Macromol. Mater. Eng.* **2013**, *298*, 896−909.
(18) Kourkoutsaki, Th.; Logakis, E.; Kroutilova, I.; Matejka, L.; Nedbal, J.; Pissis, P. Polymer dynamics in rubbery epoxy networks/polyhedral oligomeric silsesquioxanes nanocomposites. *J. Appl. Polym. Sci.* **2009**, *113*, 2569−2582.
(19) Lee, B. I.; Vergano, P. J.; Lindsay, L.; Zhang, H.; Park, H. J. Silicate modification of corn protein films. *J. Mater. Sci. Lett.* **1998**, *17*, 359−361.
(20) Frost, K.; Barthes, J.; Kaminski, D.; Lascaris, E.; Niere, J.; Shanks, R. Thermoplastic starch−silica−polyvinyl alcohol composites by reactive extrusion. *Carbohydr. Polym.* **2011**, *84*, 343−350.
(21) Matejka, L.; Dukh, O.; Brus, J.; Simonsick, W. J.; Meissner, B. Cage-like structure formation during sol-gel polymerization of glycidyloxypropyltrimethoxysilane. *J. Non-Cryst. Solids* **2000**, *270*, 34−47.
(22) Brinker, J. C.; Scherer, G. W. *Sol-Gel Science: The Physics and Chemistry of Sol-Gel Processing*; Academic Press, Inc: New York, 1990.
(23) Wellner, N.; Belton, P. S.; Tatham, A. S. Fourier transform IR spectroscopic study of hydration-induced structure changes in the solid state of ω-gliadins. *Biochem. J.* **1996**, *319*, 741−747.
(24) Wellner, N.; Mills, E. N. C.; Brownsey, G.; Wilson, R. H.; Brown, N.; Freeman, J.; Halford, N. G.; Shewry, P. R.; Belton, P. S. Changes in protein secondary structure during gluten deformation studied by dynamic fourier transform infrared spectroscopy. *Biomacromolecules* **2005**, *6*, 255−261.
(25) Mejia, C. D.; Gonzalez, D. C.; Mauer, L. J.; Campanella, O. H.; Hamaker, B. R. Increasing and stabilizing β-sheet structure of maize zein causes improvment in its rheological properties. *J. Agric. Food Chem.* **2012**, *60*, 2316−2321.
(26) Singh, N.; Georget, D. M. R.; Belton, P. S.; Barker, S. A. Physical properties of zein films containing salicylic acid and acetyl salicylic acid. *J. Cereal Sci.* **2010**, *52*, 282−287.
(27) Buonocore, G. G.; Conte, A.; Del Nobile, M. A. Use of a mathematical model to describe the water barrier properties of edible films. *J. Food Sci.* **2005**, *70*, 144−147.
(28) Pantani, R.; Sorrentino, A. Influence of cristallinity on the biodegradation rate of injection-moulded poly(lactic acid) samples in controlled composting conditions. *Polym. Degrad. Stab.* **2013**, *98*, 1089−1096.
(29) Redl, A.; Morel, M. H.; Bonicel, J.; Guilbert, S.; Vergnes, B. Rheological properties of gluten plasticized with glycerol: dependence on temperature, glycerol content and mixing conditions. *Rheol. Acta* **1999**, *38*, 311−320.
(30) Siesler, H. W. Vibrational spectroscopy of polymers. *Int. J. Polym. Anal. Charact.* **2011**, *16*, 519−541.
(31) Launer, P. J. *Infrared Analysis of Organosilicon Compounds: Spectra-Structure Correlations*; Laboratory for Materials, Inc.: Burnt Hills, NY, 1987.
(32) Wang, Y.; Filho, F. L.; Geil, P.; Padua, G. W. Effects of processing on the structure of zein/oleic acid films investigated by X-ray diffraction. *Macromol. Biosci.* **2005**, *5*, 1200−1208.
(33) Lai, H. M.; Geil, P. H.; Padua, G. W. X-Ray diffraction characterization of the structure of zein-Olic acid films. *J. Appl. Polym. Sci.* **1999**, *71*, 1267−1281.
(34) Mascia, L.; Prezzi, L.; Lavorgna, M. Peculiarities in the solvent absorption characteristics of epoxy-siloxane hybrids. *Poly Eng Sci.* **2005**, *48*, 1039−1048.

(35) Zheng, J. P.; Li, P.; Ma, L. Y.; Yao, K. D. Gelatin/montmorillonite hybrid nanocomposite. I. Preparation and properties. *J. Appl. Polym. Sci.* **2002**, *86*, 1189−1194.
(36) Verdolotti, L.; Lavorgna, M.; Di Maio, E.; Iannace, S. Hydration-induced reinforcement of rigid polyurethane cement foams: The effect of the co-continuous morphology on the thermal-oxidative stability. *Polym. Degrad. Stab.* **2013**, *98*, 64−72.
(37) Guegen, J.; Viroben, G.; Noireaux, P.; Subirade, M. Influence of plasticizers and treatments on the properties of films from pea proteins. *Ind. Crops Prod.* **1998b**, *7*, 149−157.
(38) Anker, M.; Stading, M.; Hermansson, A. M. Aging of whey protein films and the effect on mechanical and barrier properties. *J. Agric. Food Chem.* **2001**, *49*, 989−995.
(39) Orliac, O.; Rouilly, A.; Silvestre, F.; Rigal, L. Effects of various plasticizers on the mechanical properties,water resistance and aging of thermo-moulded films made fromsunflower proteinsstudied the effect of various plasticizers and aging on mechanical properties for sunflower films. *Ind. Crops Prod.* **2003**, *18*, 91−100.
(40) Lee, B. I.; Vergano, P. J.; Lindsay, L.; Zhang, H.; Park, H. J. Silicate modification of corn protein films. *J. Mater. Sci. Lett.* **1998**, *17*, 359−361.
(41) Lodha, P.; Netravali, A. N. Effect of soy protein isolate resin modifications on thei biodegradation in a compost medium. *Polym. Degrad. Stab.* **2005**, *87*, 465−477.
(42) Imam, S. H.; Gordon, S. H. Biodegradation of coproducts from industrially processed corn in a compost environment. *J. Polym. Environ.* **2002**, *10*, 147−54.